



City Research Online

## City, University of London Institutional Repository

---

**Citation:** Karim, M. R., Ahmad, H. & Rahman, B. M. (2017). All-Normal Dispersion Chalcogenide PCF for Ultraflat Mid-Infrared Supercontinuum Generation. IEEE Photonics Technology Letters, 29(21), pp. 1792-1795. doi: 10.1109/lpt.2017.2752214

This is the accepted version of the paper.

This version of the publication may differ from the final published version.

---

**Permanent repository link:** <https://openaccess.city.ac.uk/id/eprint/18497/>

**Link to published version:** <https://doi.org/10.1109/lpt.2017.2752214>

**Copyright:** City Research Online aims to make research outputs of City, University of London available to a wider audience. Copyright and Moral Rights remain with the author(s) and/or copyright holders. URLs from City Research Online may be freely distributed and linked to.

**Reuse:** Copies of full items can be used for personal research or study, educational, or not-for-profit purposes without prior permission or charge. Provided that the authors, title and full bibliographic details are credited, a hyperlink and/or URL is given for the original metadata page and the content is not changed in any way.

---

---

---

City Research Online:

<http://openaccess.city.ac.uk/>

[publications@city.ac.uk](mailto:publications@city.ac.uk)

---

# All-Normal Dispersion Chalcogenide PCF for Ultraflat Mid-Infrared Supercontinuum Generation

**Abstract**—We numerically study the dispersion-engineered chalcogenide photonic crystal fiber (PCF) which allows us to generate ultraflat broadband supercontinuum (SC) spectra in all-normal dispersion regime. A 1-cm-long chalcogenide hexagonal PCF made using  $\text{Ge}_{11.5}\text{As}_{24}\text{Se}_{64.5}$  glass pumped at  $1.55 \mu\text{m}$  produced a SC bandwidth 700 nm at a peak power of 1 kW. By shifting pump at  $2 \mu\text{m}$ , SC spectra can be extended with a bandwidth of 1900 nm at the same peak power level. In both cases, nonuniform spectral power distribution observes over the entire output bandwidth owing to the lower dispersion slope on the long wavelength side of the dispersion curve. To spanning SC further in the mid-infrared as well as to reduce the spectral asymmetry, we optimize another design for pumping at  $3.1 \mu\text{m}$  in such a way that the pump source can be employed vicinity to the peak of the dispersion curve. Employing the largest pump peak power up to 5 kW, SC can be extended up to  $6 \mu\text{m}$  (1.5 octaves) and the power distribution among the spectral components over the entire SC bandwidth can be improved significantly by this design. To enhance the spectral flatness, we optimize a second PCF geometry by reducing its pitch length and it is possible to obtain ultraflat coherent SC spanning from  $2 \mu\text{m}$  to  $5.5 \mu\text{m}$  (>1 octave) by this structure maintaining nearly symmetric power distribution between both side of its spectral components.

**Index Terms**—Nonlinear optics, Photonic crystal fiber, Chalcogenide, Dispersion, Supercontinuum generation.

## I. INTRODUCTION

Photonic crystal fibers (PCFs) are well studied and widely used optical waveguides for designing high-brightness broadband light source due to the design flexibility of their nonlinear and dispersive properties [1]. The supercontinuum (SC) light sources are designed using highly nonlinear PCF found widespread interest for the applications of frequency metrology, optical coherence tomography, telecommunication, bio-imaging, and spectroscopy [2]. The spectral broadening of SC generation relies on the interplay between various nonlinear effects and group velocity dispersion (GVD) of the optical waveguides [3]. To obtain enhanced spectral broadening, the GVD needs to be adjusted in such a way that the optical waveguide can be pumped in the anomalous dispersion regime close to the zero-dispersion wavelength (ZDW) [4]. The broadening mechanism in the case of short pump pulses mainly results from soliton dynamics and the breakup of the injected pulses through soliton fission is very sensitive to shot-to-shot input pump pulse to pulse intensity fluctuations [5]. These intensity fluctuations limit the signal-to-noise ratio in various applications including optical coherence tomography and frequency metrology [6]. The noise and amplitude fluctuation induced in spectral components can be reduced significantly by suppressing the soliton fission during SC evolution by using short waveguide design [7]. The suppression of soliton fission during pulse propagation can be achieved by obtaining the entire dispersion regime below the ZDW (GVD =

0 line) through GVD engineering of the PCF [8]. During all-normal dispersion pumping SC generation, the spectral broadening in a short waveguide is mainly dominated by self-phase modulation (SPM) and optical wave breaking (OWB) [9]. Optical waveguides optimized in all-normal dispersion enables obtaining SC spectrum with better pulse to pulse temporal coherence and spectral flatness over the entire output bandwidth but relatively narrower bandwidth is realized than anomalous dispersion regime [10].

A number of theoretical and experimental investigations on coherent SC generation was reported with pumping the silica photonic crystal fibers (PCFs) in all-normal dispersion (ANDi) region by femtosecond lasers [6], [8], [10]–[12]. However, the transmission loss of silica glass beyond  $2.2 \mu\text{m}$  limits the SC broadening in the MIR region. In recent years, chalcogenide (ChG) fibers have shown promising candidate for coherent broadband near-infrared to MIR SC generation due to their low phonon energy, higher Kerr nonlinearity and wide transparency [9]. Al-Kadry *et al.* experimentally reported the broadband coherent MIR SC generation in all-normal dispersion using 3-mm-long  $\text{As}_2\text{S}_3$  ChG microwire spanning over an octave from 960 nm to 2500 nm pumping at a wavelength of  $1.55 \mu\text{m}$  with a pulse energy of 150 pJ [5]. Liu *et al.* used 2-cm-long four-hole ChG microstructured fiber made using  $\text{AsSe}_2$  glass material to generate broadband coherent MIR SC in all-normal GVD region extending up to  $3.3 \mu\text{m}$  pumped with 200-fs pulse duration at a wavelength of  $2.7 \mu\text{m}$  with a peak power of 5.2 kW [9]. In this paper, we have demonstrated numerically a 1-cm-long dispersion-engineered highly nonlinear ChG conventional hexagonal PCF made from  $\text{Ge}_{11.5}\text{As}_{24}\text{Se}_{64.5}$  glass can be used to generate broadband ultraflat coherent MIR SC generation up to  $6 \mu\text{m}$  in all-normal dispersion employing pump at  $3.1 \mu\text{m}$  with a largest peak power of 5 kW.

## II. THEORY

The cross-section of our proposed ChG PCF is shown as an inset of Fig. 2(a) made with  $\text{Ge}_{11.5}\text{As}_{24}\text{Se}_{64.5}$  glass as a core and hexagonal lattice of air-holes running along the PCF length with central air-hole missing and consists of five rings of air-holes. We have tested the modal properties, such as effective indices, spot-size and power confinement over the wavelength for three to five rings of air holes. Modal properties almost similar, however, leakage loss shows higher for fewer rings as can be seen in Fig. 1(c). For 3 rings of air-holes, loss increases sharply after  $4 \mu\text{m}$ . The geometrical design parameter pitch ( $\Lambda$ ) and a relative hole size ( $d/\Lambda$ ) are chosen in the ranges  $\Lambda = 1.6\text{-}2.0 \mu\text{m}$  and  $d/\Lambda = 0.4\text{-}0.45$ . We optimize our ChG PCF for pumping at three different wavelengths such

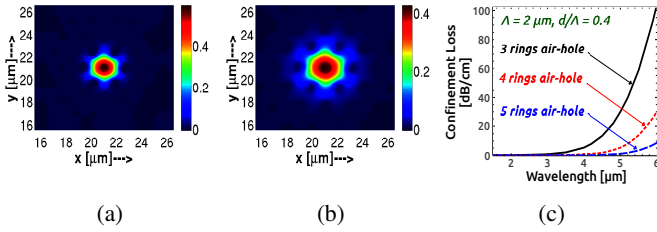


Fig. 1: (a) Field profile at  $1.55 \mu\text{m}$  for  $\Lambda = 1.6 \mu\text{m}$ ,  $d/\Lambda = 0.45$ ; (b) profile at  $3.1 \mu\text{m}$  for  $\Lambda = 2 \mu\text{m}$ ,  $d/\Lambda = 0.4$ ; and (c) confinement loss calculated for 3, 4 and 5 rings of air-holes for  $\Lambda = 2 \mu\text{m}$ ,  $d/\Lambda = 0.4$ . Both profile and confinement loss are obtained for the PCF structure of fundamental mode ( $H_x^{11}$ ).

as  $1.55 \mu\text{m}$ ,  $2 \mu\text{m}$  and  $3.1 \mu\text{m}$  separately by adjusting its  $\Lambda$  and  $d$  to obtain all-normal dispersion profile with pump wavelength vicinity to the peak of the GVD curves. By using finite-element method (FEM) based full-vectorial mode solver, we calculate the mode propagation constant of the fundamental mode over a wide range of wavelengths. We use the mode propagation constant obtained by FEM solver to calculate the effective index ( $n_{\text{eff}}$ ) of the fundamental mode. Figure 1 shows the field profiles of the fundamental mode of our proposed hexagonal PCF structure with  $\Lambda = 1.6 \mu\text{m}$ ,  $d/\Lambda = 0.45$  at a wavelength of  $1.55 \mu\text{m}$  (shown in Fig. 1a) and  $\Lambda = 2 \mu\text{m}$ ,  $d/\Lambda = 0.4$  at a wavelength of  $3.1 \mu\text{m}$  (shown in Fig. 1b). The spatial field profiles of the fundamental mode of ChG PCF in Fig. 1 at pump wavelengths exhibit excellent field confinement to the central core region which yields enhanced nonlinear interaction inside the waveguide. Utilizing the mode effective index obtained by FEM solver, the GVD parameters are calculated using the following dispersion equation [12]

$$D(\lambda) = -\frac{\lambda}{c} \frac{d^2 n_{\text{eff}}}{d\lambda^2}, \quad (1)$$

where  $c$  denotes the speed of light in the vacuum.

To study the formation of SC inside the optical waveguide, we model the pulse evolution for our proposed ChG PCF with all-normal dispersion by solving generalized nonlinear Schrödinger equation (GNLSE) [4]:

$$\begin{aligned} \frac{\partial}{\partial z} A(z, T) = & -\frac{\alpha}{2} A + \sum_{m \geq 2} \frac{i^{m+1}}{m!} \beta_m \frac{\partial^m A}{\partial T^m} \\ & + i \left( \gamma + i \frac{\alpha_2}{2A_{\text{eff}}} \right) \left( 1 + i\tau_{\text{shock}} \frac{\partial}{\partial T} \right) \\ & \times \left( A(z, T) \int_{-\infty}^{\infty} R(T') |A(z, T - T')|^2 dT' \right), \quad (2) \end{aligned}$$

where  $A(z, T)$  is the slowly varying complex electrical field envelop at a propagation distance  $z$  in a retarded reference time frame  $T = t - \beta_1 z$  moving at the group velocity  $1/\beta_1$ , the dispersion coefficients  $\beta_m$  ( $m \geq 2$ ) is the second and higher-order dispersion terms associated with the Taylor series expansion of the propagation constant  $\beta(\omega)$ ,  $\alpha$  is the linear propagation loss of the ChG PCF and  $\omega_0$  is the pump frequency. The nonlinear coefficient is defined as  $\gamma = n_2 \omega_0 / (c A_{\text{eff}})$ , where  $n_2$  is the nonlinear refractive index,  $A_{\text{eff}}$  is the effective area

of the mode at the pump angular frequency, and  $\alpha_2$  is the two-photon absorption coefficient. The time derivative in the nonlinear operator includes the effects of self-steepening and optical shock formation, which are characterized on a time scale  $\tau_{\text{shock}} = 1/\omega_0$ . The material response function  $R(t)$  includes both the instantaneous Kerr response,  $\delta(t)$ , and the delayed Raman response,  $h_R(t)$ , expressed as

$$R(t) = (1 - f_R)\delta(t) + f_R h_R(t), \quad (3)$$

$$h_R(t) = \frac{\tau_1^2 + \tau_2^2}{\tau_1 \tau_2} \exp\left(-\frac{t}{\tau_2}\right) \sin\left(\frac{t}{\tau_1}\right). \quad (4)$$

Here, the response of GeAsSe material has been predicted by considering  $f_R = 0.148$ ,  $\tau_1 = 23$ -fs and  $\tau_2 = 164.5$ -fs which are the Raman coefficients of single-peak Lorentz function fitted to  $\text{As}_2\text{Se}_3$  chalcogenide material [14].

### III. NUMERICAL RESULTS

A number of numerical simulations are carried out to design and optimize of our proposed ChG PCF such that the GVD curve can be obtained with ANDi profile which can allow us to generate broadband coherent SC generation. First, we optimize a PCF structure considering pitch  $\Lambda = 1.6$  and a relative hole-size  $d/\Lambda = 0.45$  for pumping at wavelengths of  $1.55 \mu\text{m}$  and  $2 \mu\text{m}$  separately. Figure 2(a) shows the corresponding calculated GVD curve obtained in all-normal dispersion profile. Due to having high material dispersion of ChG glass around the wavelengths of  $1.55 \mu\text{m}$  and  $2 \mu\text{m}$ , we do not able to obtain peak of the GVD curve vicinity to the pump wavelengths for this design. Then, we move to the next design and optimize a PCF structure for pumping at  $3.1 \mu\text{m}$  which is realized in tunable Raman soliton fluoride fiber lasers with the range  $2$ – $4.3 \mu\text{m}$  [15]. To obtain peak of the GVD curve vicinity to this wavelength with a smaller value of GVD, waveguide dispersion needs to be increased by adjusting the  $\Lambda$  and  $d$  of PCF. Depending on the variation of  $\Lambda$ , Fig. 2(b) shows that it is possible to obtain all-normal dispersion GVD profile for the  $\Lambda \leq 2 \mu\text{m}$ , while above this value the GVD curve extends into the anomalous dispersion region. It is also apparent from this figure that GVD curve slightly moves left to right with the increasing of PCF pitch length.

For studying SC generation in all-normal dispersion profile, we numerically solve GNLSE Eq. (2) for single-polarization

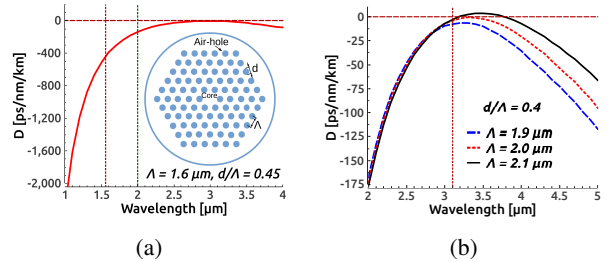


Fig. 2: GVD curves for the ChG hexagonal PCF tailored for pumping at wavelengths of (a)  $1.55$  and  $2 \mu\text{m}$ , (b)  $3.1 \mu\text{m}$ . Vertical dotted lines indicate pump wavelengths. PCF geometry is shown as an inset of Fig. a.

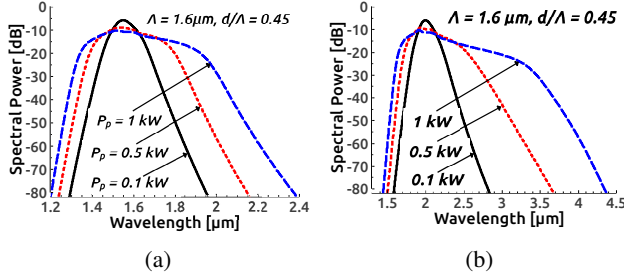


Fig. 3: Output SC spectra at pump wavelengths of (a) 1.55  $\mu\text{m}$  and (b) 2  $\mu\text{m}$  corresponding to the GVD curve shown in Fig. 2(a) for the PCF structure of  $\Lambda = 1.6$ ,  $d/\Lambda = 0.45$ .

with the split-step Fourier method. Initially, a sech pulse of 50-fs duration (FWHM) at a pump wavelength of 1.55  $\mu\text{m}$  was launched with peak power between 100 and 1000 W for numerical simulations. We included a wavelength independent propagation loss of 3.2 dB/cm at this wavelength. The  $n_2$  and  $\alpha_2$ , which have been measured at a wavelength of 1.55  $\mu\text{m}$  by Wang *et al.* [13] using z-scan technique, are assumed to be  $7.33 \times 10^{-18} \text{ m}^2/\text{W}$  and  $7.88 \times 10^{-14} \text{ m/W}$ , respectively. Using FEM solver, we calculate  $A_{\text{eff}} = 3.43 \mu\text{m}^2$  which yields  $\gamma = 8.66 \text{ /W/m}$  at a wavelength of 1.55  $\mu\text{m}$ . Since this  $A_{\text{eff}}$  is smaller than the mode effective area of typical single mode fiber, so the coupling loss can be higher. Tapered spot-size converter can be used to reduce the loss. The GVD parameter is calculated as  $-444 \text{ ps/nm/km}$  at this wavelength. Figure 3(a) shows the predicted SC spectra for a ChG PCF optimized for a  $\Lambda = 1.6 \mu\text{m}$  and a relative hole size ratio  $d/\Lambda = 0.45$ . A broadband flat SC spectrum covering the wavelength from 1350 to 1850 nm with a bandwidth of 500 nm wide can be obtained with a peak power of 500 W. Bandwidth can be enhanced up to 700 nm spanning the spectrum up to 2000 nm by increasing peak power at a level of 1 kW. In this case, relatively the large value of GVD parameter at pump wavelength limits the spectral broadening significantly. On the other hand, the lower dispersion slope at long wavelength leads to increased spectral asymmetry between the short and long wavelength components.

To enhance the spectral symmetry, we shift the pump at a lower dispersion slope with a wavelength of 2  $\mu\text{m}$  for the same PCF geometry where GVD parameter measured at a value of  $-138 \text{ ps/nm/km}$  as shown in Fig. 2(a). Employing FEM solver, we evaluate  $A_{\text{eff}} = 3.65 \mu\text{m}^2$  which results  $\gamma = 6.3 \text{ /W/m}$  at this wavelength. Figure 3(b) shows broadband coherent SC spectra after carrying out simulations pumping at 2  $\mu\text{m}$  with peak power range 0.1-1 kW. The spectra has SPM dominated and the bandwidth achieved in this case are 700 nm and 1250 nm covering the wavelength ranges 1650–2750 nm and 1600–3500 nm at peak power levels of 0.5 kW and 1 kW, respectively. Since the GVD curve still having asymmetric around the pump wavelength, it leads to maintain spectral asymmetry over the entire SC bandwidth achieved at the PCF output.

To further extend the SC spectra in the MIR with increasing the spectral symmetry, we optimize a next PCF geometry with  $\Lambda = 2$ ,  $d/\Lambda = 0.4$  for pumping at 3.1  $\mu\text{m}$ . The  $\alpha$  of the ChG

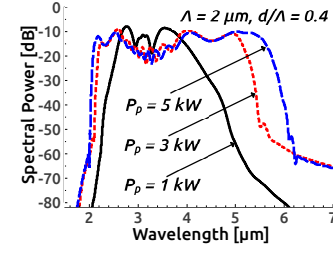


Fig. 4: Output SC spectra corresponding to the GVD curve obtained in Fig. 2(b) (dotted red curve) for the PCF structure of  $\Lambda = 2$ ,  $d/\Lambda = 0.4$  at a pump wavelength of 3.1  $\mu\text{m}$  with a peak power in the range 1-5 kW.

material at a pump wavelength is assumed to be 0.5 dB/cm though the loss may be negligible in short waveguide design. The value of  $n_2$  makes half at 3.1  $\mu\text{m}$  from its earlier value mentioned at 1.55  $\mu\text{m}$ . We evaluate  $A_{\text{eff}} = 7.07 \mu\text{m}^2$  at a pump wavelength to calculate  $\gamma = 1.05 \text{ /W/m}$  as Heidt *et al.* [8] suggested constant  $\gamma$  achieves a better fit than  $A_{\text{eff}}$  dependent  $n_2$ . The GVD parameter  $D = -3.92 \text{ ps/nm/km}$  measured at this wavelength (dotted red curve in Fig. 2b). Figure 4 shows the obtained broadband coherent SC spectra after launching a sech pulse of 100-fs duration with peak power in the range 1-5 kW. A broadband coherent SC spectrum can be spanned up to 4.4  $\mu\text{m}$  and 5.4  $\mu\text{m}$  with a peak power of 1 kW and 3 kW, respectively. Further spectral broadening can be obtained up to 6  $\mu\text{m}$  if we raise the peak power level at 5 kW. Since the nonlinearity falls in longer pump wavelength owing to larger mode effective area, so the input pump power has been increased with pump wavelength to achieve sufficient MIR SC extension at the PCF output. In this case, significant improvement in spectral symmetry can be observed between both sides of the pump wavelength than earlier designs.

To obtain the SC spectrum with reduced fluctuation, we optimize another geometry containing  $\Lambda = 1.9$  and  $d/\Lambda = 0.4$  for pumping at the same wavelength keeping all other parameters same as before. We calculate  $A_{\text{eff}} = 6.58 \mu\text{m}^2$  at a pump wavelength which yields  $\gamma = 1.13 \text{ /W/m}$ . The GVD calculated at this wavelength is  $-7.40 \text{ ps/nm/km}$ . Figure 5(a) shows the broadband coherent SC spectrum spanned up to 5.5  $\mu\text{m}$  and its corresponding spectral density, spectrogram and coherence are shown in Figs. 5(b)-5(d), respectively. It is apparent from Fig. 5(a) that spectral flatness can be increased by decreasing  $\Lambda$  from 2  $\mu\text{m}$  to 1.9  $\mu\text{m}$ . In this case, somewhat bandwidth reduction observed due to having higher GVD value at the pump wavelength. However, in the case of both PCF structures optimized with  $\Lambda$  of 1.9  $\mu\text{m}$  and 2  $\mu\text{m}$ , spectral uniformity remains unchanged over the entire SC bandwidth in spite of each having different GVD value at pump wavelength.

The spectral broadening mechanism in all-normal dispersion can be described from the SC evolution shown in Figs. 5(b)-5(c). At the beginning, pump pulse is broadened due to the SPM around the pump wavelength symmetrically. Then, as can be seen in Fig. 5(b) the effect of OWB starts to be apparent after 3.6 mm of propagation inducing two side lobes generating new frequencies on the both side of the pump wavelength. The new frequencies on side lobes rapidly gain intensity

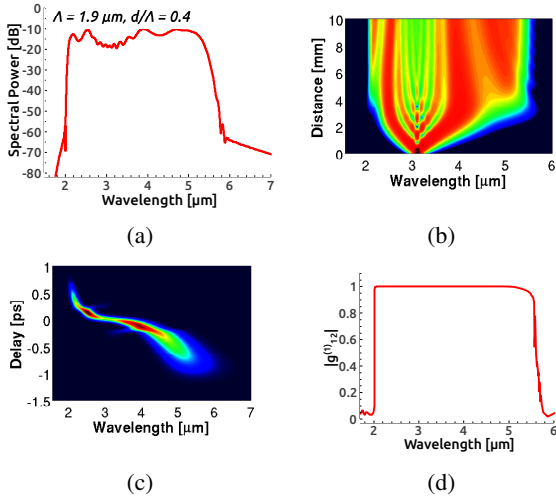


Fig. 5: SC at PCF output (a) spectrum; (b) spectral density evolution; (c) spectrogram; and (d) the corresponding degree of coherence for the GVD curve shown in Fig. 2(b) (dashed blue curve) for the PCF structure of  $\Lambda = 1.9$ ,  $d/\Lambda = 0.4$  at a pump pulse launched at  $3.1 \mu\text{m}$  with a peak power of 5 kW.

by depleting energy from SPM induced peaks resulting the spectral recoiling which may seem to limit the obtainable SC bandwidth. However, owing to merging the side lobe spectral components with the SPM induced peaks eventually enhance the total obtainable bandwidth at the PCF output.

The coherence properties of our proposed geometries can be tested by using the coherence measurement procedure described in [2], [4]. Figure 5(d), which is entirely coherent over the whole SC bandwidth obtained at the PCF output, illustrates the modulus of the complex 1st degree of coherence calculated using ensemble average of twenty pairs of independent SC spectra with different noise seeds for the PCF structure of  $\Lambda = 1.9 \mu\text{m}$ ,  $d/\Lambda = 0.4$ .

#### IV. CONCLUSION

In this paper, we have demonstrated numerically a 1-cm-long dispersion-engineered chalcogenide conventional hexagonal PCF which allow us to generate broadband coherent MIR SC spectra in all-normal dispersion regime. Detail approach to achieve broadband ultraflat coherent SC generation in the absence of solitonic fission inside the optical waveguide has been demonstrated. By optimizing ChG PCF for pumping at three different wavelengths such as  $1.55 \mu\text{m}$ ,  $2 \mu\text{m}$  and  $3.1 \mu\text{m}$ , broadband ultraflat SC can be generated from near-IR to MIR region. For pumping at wavelengths of  $1.55$  and  $2 \mu\text{m}$ , we optimize a PCF by varying its structural parameters and it is possible to obtain SC bandwidth of 700 nm and 1250 nm at peak power of 1 kW by this design. In both cases, the output bandwidth is limited due to large normal dispersion at the pump wavelength. Moreover, low GVD value after the peak of the GVD curve leads to decreased spectral symmetry in both sides of the pump wavelengths.

To increase spectral symmetry with further extending the SC into the MIR, we optimize two more PCF geometries by adjusting their structural parameters for pumping at  $3.1 \mu\text{m}$ . A

broadband ultraflat MIR SC can be realized up to  $6 \mu\text{m}$  with a largest peak power of 5 kW by the 1st geometry. On the other hand, by optimizing a 2nd PCF with having relatively a higher GVD, a broadband coherent MIR SC can be predicted up to  $5.5 \mu\text{m}$  at the same power level with increased spectral flatness than earlier design. In both cases, nearly symmetric spectra realized over the entire SC bandwidth at the PCF output.

#### REFERENCES

- [1] J. M. Dudley and J. R. Taylor, "Ten years of nonlinear optics in photonic crystal fiber," *Nat. Photonics*, vol. 3, pp. 85–90, 2009.
- [2] A. M. Heidt "Pulse preserving flat-top supercontinuum generation in all-normal dispersion photonic crystal fibers," *J. Opt. Soc. Am. B*, vol. 27, no. 3, pp. 550–559, Mar. 2010.
- [3] G. P. Agrawal, *Nonlinear Fiber Optics 5th ed.* (Academic, San Diego, California, 2013).
- [4] J. M. Dudley, G. Genty, and S. Coen, "Supercontinuum generation in photonic crystal fiber," *Rev. Mod. Phys.*, vol. 78, no. 4, pp. 1135–1184, Dec. 2006.
- [5] A. Al-Kadry, L. Li, M. E. Amraoui, T. North, Y. Messaddeq, and M. Rochette, "Broadband supercontinuum generation in all-normal dispersion chalcogenide nanowires," *Opt. Letter*, vol. 40, no. 20, pp. 4687–4690, Oct. 2015.
- [6] L. E. Hooper, P.J. Mosley, A. C. Muir, W. J. Wadsworth, and J. C. Knight, "Coherent supercontinuum generation in photonic crystal fiber with all-normal group velocity dispersion," *Opt. Express*, vol. 19, no. 6, pp. 4902–4907, Mar. 2011.
- [7] C. Finot, B. Kibler, L. Provost, and S. Wabnitz, "Beneficial impact of wave-breaking for coherent continuum formation in normally dispersive nonlinear fibers," *J. Opt. Soc. Am. B*, vol. 25, no. 11, pp. 1938–1337, Nov. 2008.
- [8] A. M. Heidt, A. Hartung, G. W. Bosman, P. Krok, E. G. Rohwer, H. Schwoerer, and H. Bartelt, "Coherent octave spanning near-infrared and visible supercontinuum generation in all-normal dispersion photonic crystal fibers," *Opt. Express*, vol. 19, no. 4, pp. 3775–3778, Feb. 2011.
- [9] L. Liu, T. Cheng, K. Nagasaka, H. Tong, G. Qin, T. Suzuki, and Y. Ohishi, "Coherent mid-infrared supercontinuum generation in all-solid chalcogenide microstructured fibers with all-normal dispersion," *Opt. Letter*, vol. 41, no. 2, pp. 392–395, Jan. 2016.
- [10] G. Stepniowski, M. Klimczak, H. Bookey, B. Siwicki, D. Pysz, R. Stepien, A. K. Kar, A. J. Waddie, M. R. Taghizadeh, and R. Buczynski, "Broadband supercontinuum generation in normal dispersion all-solid photonic crystal fiber pumped near 1300 nm," *Laser Phys. Lett.*, **11**, pp. 055103, Mar. 2014.
- [11] B. Siwicki, M. Klimczak, R. Stepien, and R. Buczynski, "Supercontinuum generation enhancement in all-solid all-normal dispersion soft glass photonic crystal fiber pumped at 1550 nm," *Opt. Fiber Tech.*, vol. 25, pp. 64–71, Oct. 2015.
- [12] Z. Guo, J. Yuan, C. Yu, X. Sang, K. Wang, B. Yan, L. Li, S. Kang, and X. Kang, "Highly coherent supercontinuum generation in the normal dispersion liquid-core photonic crystal fiber," *Prog. in Elec. Res.*, vol. 48, pp. 67–76, May. 2016.
- [13] T. Wang, X. Gai, W. Wei, R. Wang, Z. Yang, X. Shen, S. Madden, and B. Luther-Davies, "Systematic z-scan measurements of the third order nonlinearity of chalcogenide glasses," *Opt. Mater. Express*, vol. 4(5), pp. 1011-1022, 2014.
- [14] A. B. Salem, R. Cherif, and M. Zghal, "Raman response of a highly nonlinear  $\text{As}_2\text{Se}_3$ -based chalcogenide photonic crystal fiber," in PIERS Proceedings, Marrakesh, Morocco, pp. 1256, March 20–23, 2011.
- [15] Y. Tang, L. G. Wright, K. Charan, T. Wang, C. Xu, and F. W. Wise, "Generation of intense 100-fs solitons tunable from 2 to  $4.3 \mu\text{m}$  in fluoride fiber," *Optica*, vol. 3, pp. 948-951, 2016.